

Acetic Acid Formation by Selective Aerobic Oxidation of Aqueous Ethanol over Heterogeneous Ruthenium Catalysts

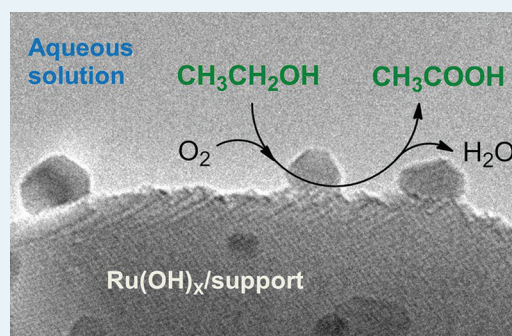
Yury Y. Gorbanev,[†] Søren Kegnæs,[†] Christopher W. Hanning,[†] Thomas W. Hansen,[‡] and Anders Riisager^{*,†}

[†]Centre for Catalysis and Sustainable Chemistry, Department of Chemistry, and [‡]Center for Electron Nanoscopy, Technical University of Denmark, DK-2800 Kgs. Lyngby, Denmark

Supporting Information

ABSTRACT: Heterogeneous catalyst systems comprising ruthenium hydroxide supported on different carrier materials, titania, alumina, ceria, and spinel (MgAl_2O_4), were applied in selective aerobic oxidation ethanol to form acetic acid, an important bulk chemical and food ingredient. The catalysts were characterized by X-ray powder diffraction (XRPD), transmission electron microscopy (TEM), energy dispersive spectroscopy (EDS), and nitrogen physisorption and utilized in the oxidation of 2.5–50 wt % aqueous ethanol solutions at elevated temperatures and pressures. The effects of Ru metal loading, pretreatment of catalysts, oxidant pressure, reaction temperature, and substrate concentration were investigated. Quantitative yield of acetic acid was obtained with 1.2 wt % $\text{Ru}(\text{OH})_x/\text{CeO}_2$ under optimized conditions (150 °C, 10 bar O_2 , 12 h of reaction time, 0.23 mol % Ru to substrate).

KEYWORDS: ethanol, acetic acid, oxidation, heterogeneous catalysis, ruthenium hydroxide catalysts



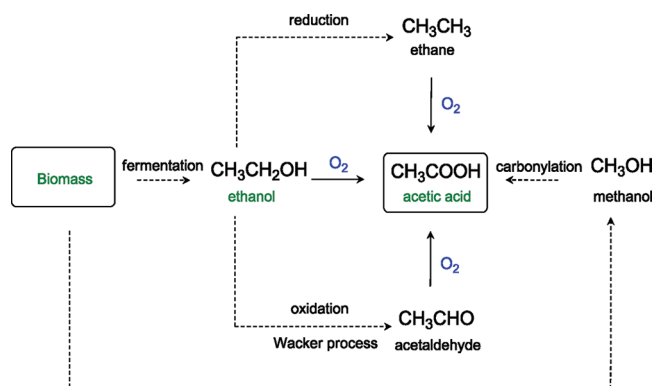
1. INTRODUCTION

Acetic acid is a highly important commodity chemical with a current annual production of approximately 8.5 million tonnes and annual growth rate of roughly 1%.¹ Traditionally, acetic acid has been derived from ethanol via fermentation, a production route that is still used today to make vinegar (i.e., aqueous acetic acid).² Since the late 1990s, production of biomass-derived ethanol or “bioethanol” has increased dramatically.³ So far the main utilization of bioethanol has been as fuel additive. However, ethanol is a low value bulk chemical with potential to be a sustainable chemical feedstock when upgraded to other higher value products like acetic acid.⁴ Although such “bioacetic acid” would only make up a small volume of the total annual acetic acid production (i.e., 0.8 million tons per year),² this is still a significant volume positioning this production route in the lower end of the bulk chemical scale production.

As an alternative to fermentation of ethanol, various chemical pathways to aqueous acetic acid have already been reported in the literature, including aerobic oxidation reactions. Molecular oxygen is a highly desired oxidant, since it is photosynthesized by plants, produces little waste, is inexpensive, and has larger atom efficiency than other oxidants.⁵ Conversion of biomass or biomass-derived chemicals with such abundant oxidant as oxygen for the production of chemicals would thus allow combining a renewable feedstock with a renewable oxidant.⁶

An obvious route to acetic acid is via the aerobic oxidation of ethyl species⁷ which has been demonstrated with ethane⁸ and acetaldehyde⁹ besides ethanol (Scheme 1). These methods

Scheme 1. Possible Routes for the Production of Acetic Acid from Biomass



have, however, only been shown on a laboratory scale and not successfully scaled up to industrial levels,⁸ though the possibility of obtaining acetic acid from biomass via bioethanol would be an attractive route that is not based on petrochemicals like the current large scale productions via methanol carbonylation⁹ or acetaldehyde oxidation (Wacker process).⁸

For the oxidation of ethanol, studies have shown that supported gold,^{4,10–12} copper/copper–chromium oxides,¹³

Received: October 26, 2011

Revised: February 27, 2012

Published: February 28, 2012

molybdenum, vanadium, niobium mixed oxides,¹⁴ palladium,^{15–17} and platinum¹⁸ catalysts can be used. Hence, Rajesh et al.¹³ achieved yields of acetaldehyde up to 27% by oxidation using either copper or copper–chromium catalysts supported on γ -alumina. Li et al.¹⁴ showed that supported mixed oxides containing molybdenum, vanadium and niobium provided 100% ethanol conversion combined with a 95% selectivity toward acetic acid. ten Brink and co-workers¹⁵ demonstrated use of a homogeneous palladium catalyst in a biphasic system for the oxidation of both primary and secondary alcohols in aqueous medium. Here conversions higher than 90% for a large variety of substrates were obtained with isolated yields of the corresponding ketone, aldehyde, or carboxylic acid above 80%. Nishimura et al.¹⁶ made use of supported palladium catalyst to perform the oxidation of primary and secondary alcohols to aldehydes and ketones. Also here high conversions were combined with high isolated yields (>95% and >85%, respectively).

Gold catalysts supported on silica, titania, ceria, zinc oxide, and niobium oxide have been explored by various research groups for the oxidation of ethanol in both liquid and gas phase, providing high conversion and selectivity toward acetic acid. Most of these results are summarized in the recent review by Haruta et al.¹⁹ We have previously reported the selective oxidation of ethanol to acetic acid in aqueous solution utilizing Au/MgAl₂O₄ and Au/TiO₂ catalysts and dioxygen.^{20,21} Here, we show the superior performance of supported Ru(OH)_x as a catalyst for this process.

Catalysts composed of Ru(OH)_x supported on alumina, ceria, and titania were previously reported by Mizuno and co-workers^{22–26} and Zhang et al.²⁷ to be efficient catalysts for aerobic oxidation of alcohols to aldehydes and ketones, and amines to nitriles. In the present work, Ru(OH)_x supported on TiO₂, Al₂O₃, CeO₂, or MgAl₂O₄ catalysts are described for catalytic aerobic oxidation of ethanol to acetic acid in aqueous solutions with moderate to excellent yields at relatively benign reaction conditions.

2. EXPERIMENTAL SECTION

2.1. Materials. Ethanol (99.9%, Kemetyl A/S), acetaldehyde (>99.5%, Sigma-Aldrich), acetic acid (99.8%, Riedel-de Haën AG), ruthenium(III) chloride (purum, 40–42% Ru, Sigma-Aldrich), titanium oxide (anatase, 99.7%, Sigma-Aldrich), MgAl₂O₄ (spinel, purum, Sigma-Aldrich), γ -aluminum oxide (>99.9%, Sigma-Aldrich), cerium oxide (99.5%, Alfa Aesar), sodium hydroxide (>98%, Sigma-Aldrich), and dioxygen (99.5%, Air Liquide Denmark) were all used as received.

2.2. Catalyst Preparation and Characterization. The catalysts were prepared by a method adapted from literature.^{22–26} Support (Al₂O₃, CeO₂, MgAl₂O₄ or TiO₂) in the amounts of 2.44, 4.88, 9.76, or 19.52 g were added to 143 mL of 8.3 mM aqueous RuCl₃ solution (1.19 mmol Ru). After stirring for 15 min, 28 mL of 1 M NaOH solution was added, and the mixtures were stirred for 18 h. Then the catalysts were filtered off, washed thoroughly with water until neutral reaction (colorless filtrates suggested absence of ruthenium ions), and dried at 140 °C for 40 h resulting in catalysts with optimally 4.7, 2.4, 1.2, and 0.6 wt % Ru, respectively. For the study of heat treatment effects, catalysts were subsequently calcined at 170 or 450 °C in air for 18 h.

Unsupported ruthenium hydroxide was prepared similarly to described above, via the precipitation of Ru(OH)_x from aqueous solution of RuCl₃ with added 1 M NaOH. The precipitate was filtered off, washed, and dried at 140 °C.

Surface areas were determined by nitrogen physisorption measurements at liquid nitrogen temperature on a Micro-metrics ASAP 2020 apparatus. The samples were outgassed in vacuum at 150 °C for 6 h prior to measurements. The total surface areas were calculated according to the Brunauer–Emmett–Teller (BET) method.

Transmission electron microscopy (TEM) images were acquired using a FEI Tecnai Transmission Electron Microscope operated at 200 kV by dispersing samples on a lacy amorphous carbon support film.

Energy dispersive spectroscopy (EDS) analysis was performed using an adjacent Oxford INCA system. The presented Ru metal contents were calculated from the EDS results and are averaged values based on 3–5 measurements on chosen spots of the analyzed samples after exclusion of extraordinary high or low values (not exceeding a two-fold amount).

X-ray powder diffraction (XRPD) patterns were recorded using a Huber G670 powder diffractometer (Cu–K α radiation, $\lambda = 1.54056$ nm) in the 2θ interval 5–100°.

2.3. Oxidation Reactions. Oxidations were carried out in stirred Parr autoclaves equipped with internal thermocontrol (T316 steel, Teflon beaker insert, 100 mL). In each reaction the autoclave was charged with 10 g of 2.5–50 wt % aqueous ethanol solution.

The supported 0.6–4.7 wt % Ru(OH)_x catalyst (weight percentage given on Ru metal basis) was added (0.05–0.42 g, 0.012–0.05 mmol Ru) to the solution, and the autoclave was pressurized with dioxygen (10–30 bar, ca. 16–48 mmol) and maintained at a fixed temperature between 125 and 250 °C for a given period of time under stirring (500 rpm). After the reaction, the autoclave was rapidly cooled to room temperature. The reaction mixture was then filtered and analyzed using HPLC (Agilent Technologies 1200 series, Aminex HPX-87H column from Bio-Rad, 300 mm \times 7.8 mm \times 9 μ m, flow 0.6 mL/min, solvent 5 mM H₂SO₄, temperature 60 °C) and/or GC-MS (GC Agilent Technologies 6850 coupled with MS Agilent Technologies 5975C, HP-5MS column from J & W Scientific, 30 m \times 0.25 mm \times 0.25 μ m, 5 mol % phenylmethylpolysiloxane, flow gas He). In all figures where the product distribution is shown as a function of time each data point corresponds to an individual reaction run.

Reaction with the unsupported Ru(OH)_x was performed in a similar way as above. However, here the reaction was up-scaled using 100 g of 5 wt % aqueous ethanol with 25 mg of Ru(OH)_x catalyst.

In a leaching test, the reaction was carried out at 150 °C under 10 bar of O₂ for 1 h. Then the catalyst was filtered off, and the filtrate poured back into the autoclave. The autoclave was then repressurized with 10 bar O₂, and the reaction continued for another 2 h. Finally the reaction mixture was analyzed as described above. Inductively coupled plasma (ICP) analysis (Perkin-Elmer ELAN 6000 with cross-flow nebulizer and argon plasma) was performed on diluted postreaction mixtures and quantified with ICP standard solutions.

3. RESULTS AND DISCUSSION

3.1. Catalyst Characterization. XRPD patterns of all the used catalysts are shown in the Supporting Information (Figure S1). Only diffractions characteristic of the support materials were identified and no indication of crystalline ruthenium containing species was observed. Electron paramagnetic resonance (EPR) analysis suggested the supported Ru(OH)_x

catalysts consist of amorphous mixed Ru^{4+} and Ru^{3+} species, as described elsewhere.³⁰

Representative TEM images of the prepared $\text{Ru}(\text{OH})_x/\text{CeO}_2$ catalysts are presented in Figure 1. In the images ruthenium

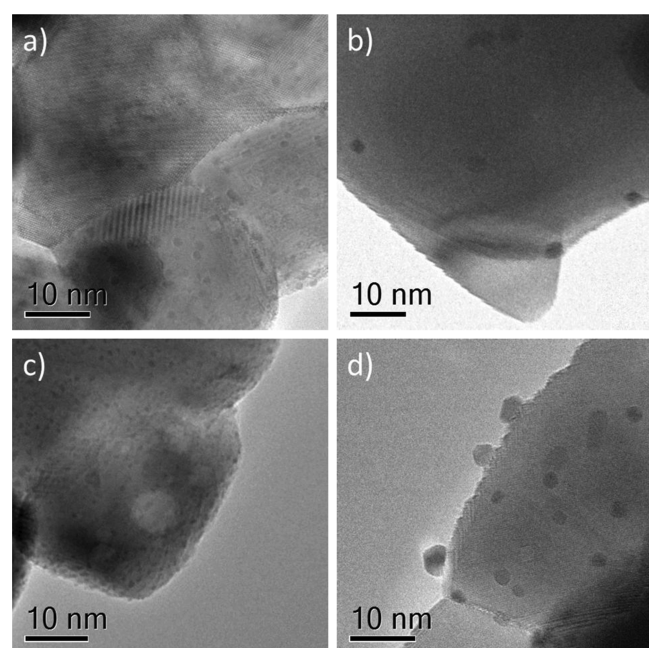


Figure 1. High-resolution TEM images of the (a) 0.6 wt %, (b) 1.2 wt %, (c) 2.4 wt %, and (d) 4.7 wt % $\text{Ru}(\text{OH})_x/\text{CeO}_2$ catalysts.

hydroxide particle agglomerates of different size are observed, and the sizes are compiled in Table 1. TEM images of the

Table 1. Characteristics of Supports and Supported $\text{Ru}(\text{OH})_x$ Catalysts

entry	material	BET surface area (m^2/g)	Ru content ^a (wt %)	particle size ^b (nm)
1	TiO_2	123		
2	2.4 wt % $\text{Ru}(\text{OH})_x/\text{TiO}_2$	128	2.3	n/a
3	Al_2O_3	149		
4	2.4 wt % $\text{Ru}(\text{OH})_x/\text{Al}_2\text{O}_3$	145	2.2	n/a
5	MgAl_2O_4	63		
6	1.2 wt % $\text{Ru}(\text{OH})_x/\text{MgAl}_2\text{O}_4$	54	1.3	0.5–2
7	2.4 wt % $\text{Ru}(\text{OH})_x/\text{MgAl}_2\text{O}_4$	53	2.4	n/a
8	CeO_2	62		
9	0.6 wt % $\text{Ru}(\text{OH})_x/\text{CeO}_2$	8	0.8	0.5–2
10	1.2 wt % $\text{Ru}(\text{OH})_x/\text{CeO}_2$	8	1.3	0.6–2
11	2.4 wt % $\text{Ru}(\text{OH})_x/\text{CeO}_2$	8	2.3	0.8–3.5
12	4.7 wt % $\text{Ru}(\text{OH})_x/\text{CeO}_2$	8	4.6	1.5–6

^aBased on Ru:Ti, Ru:Al, Ru:Ce atomic ratios provided by EDS (average for the analyzed sample). ^bDetermined from TEM images.

titania- and spinel-supported catalysts are shown in the Supporting Information (Figure S2).

The data obtained from EDS analysis and BET surface areas of the applied support materials and the prepared catalyst samples are listed in Table 1. As seen from the data, the experimental ruthenium contents determined by EDS were in good accordance with the calculated amounts for the catalysts.

The nitrogen physisorption analysis revealed a moderate change in BET surface areas when the ruthenium species were

deposited on TiO_2 , Al_2O_3 , and MgAl_2O_4 supports (Table 1, entries 1–7). In contrast, the decrease in the BET surface area of $\text{Ru}(\text{OH})_x$ catalysts supported on CeO_2 compared to pure CeO_2 was much more pronounced (Table 1, entries 8–12). Moreover, the particle sizes of the deposits on 0.6, 1.2, 2.4, and 4.7 wt % $\text{Ru}(\text{OH})_x/\text{CeO}_2$ catalysts increased with increasing ruthenium loading (Table 1, entries 9–12). A few anomalously large agglomerates of ruthenium species were observed in TEM on the surface of cerium oxide. In contrast, the results from EDS analysis of the catalyst supported on spinel (Table 1, entries 6 and 7) revealed small variation in the amount of determined ruthenium, thus suggesting an improved dispersion of active species on the surface of spinel. With respect to catalytic performance, the contribution of the agglomerates was expected to be negligible, since the surface area provided by these few large particles was insignificant compared to the collective surface area of the smaller particles.

3.2. Screening of Catalysts with Different Supports. In previous work, aerobic oxidation of bioethanol (i.e., 5 wt % ethanol solution in water) to acetic acid was performed with spinel- and titania-supported gold nanoparticle catalysts at elevated temperatures and high pressures.^{20,21} In the present work, we investigated the aforementioned oxidation with $\text{Ru}(\text{OH})_x$ supported on titania, alumina, spinel, and ceria as catalysts (Table 2). Spinel, titania, and ceria are water-stable and attractive supports for various catalytic reactions, and were also applied in our previous aerobic oxidation studies with biorenewables.^{28–31}

As seen from the obtained results, all four tested supported catalysts exhibited high activity in the aerobic oxidation of ethanol. When tested at 175 °C, close to full conversion and yields above 85% of acetic acid at 30 bar of oxygen after 3 h of reaction were found. The efficiency of the titania- and alumina-supported catalysts proved to be comparable, whereas $\text{Ru}(\text{OH})_x/\text{MgAl}_2\text{O}_4$ was slightly more efficient (Table 2, entries 1, 3, and 4; entries 2 and 5). Interestingly, $\text{Ru}(\text{OH})_x/\text{CeO}_2$ showed superior catalytic performance in the oxidation reaction, especially at lower temperature. In fact, even at a temperature of 125 °C the product yields in the reaction with $\text{Ru}(\text{OH})_x/\text{CeO}_2$ catalyst (Table 2, entry 7) were higher than the respective yields at 150 °C for the other supports (Table 2, entries 1, 3, and 4). Hence, the Al_2O_3 -supported catalyst, which provided excellent selectivities and yields for the oxidation of alcohols in organic solvents,²² did not exhibit such superior performance in the present aqueous system. For comparison, an experiment with unsupported $\text{Ru}(\text{OH})_x$ catalyst was performed resulting in significantly lower substrate conversion and product yields (Table 2, entry 10).

A more comprehensive study under lower reaction pressure was performed for two catalysts (ceria and spinel) while running reactions long enough to achieve high yields under these conditions (Table 3).

The results presented in Table 3 show that ceria-supported ruthenium catalyst performed more efficiently than $\text{Ru}(\text{OH})_x/\text{MgAl}_2\text{O}_4$ at the same reaction conditions, that is, 10 bar of dioxygen and 150 °C (Table 3, entries 2 and 3). The results of the temperature variation (entries 4–6) further showed that an acetic acid yield above 80% was observed already after only 3 h of reaction time at 200 °C using the $\text{Ru}(\text{OH})_x/\text{CeO}_2$ catalyst. However, an increased temperature of 250 °C resulted in a lower yield of acetic acid (and lower overall carbon mass balance), most likely because of the decomposition of the aqueous acetic acid over the ruthenium catalyst, similarly to

Table 2. Product Distribution in the Aerobic Oxidation of Aqueous Ethanol with Supported 2.4 wt % Ru(OH)_x Catalysts at Different Temperatures^a

entry	catalyst	temperature (°C)	conversion (%)	yield (%)	
				CH ₃ CHO	CH ₃ COOH
1	Ru(OH) _x /TiO ₂	150	76	26	37
2	Ru(OH) _x /TiO ₂	175	96	6	86
3	Ru(OH) _x /Al ₂ O ₃	150	79	35	39
4	Ru(OH) _x /MgAl ₂ O ₄	150	82	30	48
5	Ru(OH) _x /MgAl ₂ O ₄	175	>99	0	96
6	Ru(OH) _x /MgAl ₂ O ₄	200	>99	0	95
7	Ru(OH) _x /CeO ₂	125	80	17	62
8	Ru(OH) _x /CeO ₂	150	92	11	78
9	Ru(OH) _x /CeO ₂	175	>99	0	96
10 ^b	Ru(OH) _x	150	8	4	3

^aReaction conditions: 10 g of 5 wt % aqueous ethanol, 0.23 mol % Ru, 30 bar O₂, 3 h of reaction time. ^bUnsupported Ru(OH)_x.

Table 3. Product Distribution in the Aerobic Oxidation of Aqueous Ethanol with Supported 2.4 wt % Ru(OH)_x Catalysts^a

entry	catalyst	reaction time (hours)	temperature (°C)	conversion (%)	yield (%)	
					CH ₃ CHO	CH ₃ COOH
1	Ru(OH) _x /CeO ₂	20	125	58	27	30
2	Ru(OH) _x /CeO ₂	20	150	>99	0	>99
3	Ru(OH) _x /MgAl ₂ O ₄	20	150	95	6	88
4	Ru(OH) _x /CeO ₂	3	150	63	30	31
5	Ru(OH) _x /CeO ₂	3	200	94	10	83
6	Ru(OH) _x /CeO ₂	3	250	>99	7	62

^aReaction conditions: 10 g of 5 wt % aqueous ethanol, 0.23 mol % Ru, 10 bar of O₂.

that reported by Imamura et al.³² In their study, decomposition was found when oxidation of aqueous acetic acid was performed over a catalyst composed of RuO₂ supported on CeO₂ at 200 °C under 30 bar of O₂/N₂. Notably, in our work no significant overoxidation to CO₂ or other product degradation seemed to occur with Ru(OH)_x/CeO₂ catalyst even at 200 °C, where the carbon mass balance still remained high (i.e., >95%). Decreasing the temperature to 125 °C significantly affected the rate of the reaction (as expected), providing only about 30% acetic acid at 60% conversion of ethanol after 20 h (Table 3, entry 1). Thus, overall the Ru(OH)_x/CeO₂ catalyst proved to be superior compared to the other examined catalysts in the temperature range 125–200 °C where overoxidation was not observed.

Figure 2 presents product yields as a function of reaction time in the oxidation reaction of 5 wt % aqueous ethanol solution with 2.4 wt % Ru(OH)_x/CeO₂ under 10 bar of O₂ at 150 and 200 °C, respectively. The data confirms that the initially formed acetaldehyde was oxidized into acetic acid as the reaction progressed. Notably, acetaldehyde was thus an intermediate oxidation product under these conditions, rather than a final product as in the study reported by Liu et al.³³ where ethanol was oxidized to acetaldehyde at low temperatures using RuO₂ supported on tin, titanium, aluminum, zirconium oxides, or silica. At 200 °C the aldehyde oxidation occurred relatively faster than at 150 °C, making acetic acid the major product even already after 1 h of reaction time. In fact, a reaction pathway involving initial formation of acetaldehyde via formation of alkoxide species followed by β-hydride elimination is in good accordance with the mechanism suggested by Mizuno and co-workers^{25,26,34} for oxidation of alcohols to aldehydes and ketones over supported Ru(OH)_x catalysts, though the proposed reaction mechanism^{25,26} and associated ab initio calculations³⁴ focusing on a catalyst model comprised only of

the Ru³⁺ oxidation state did not include aqueous media. Thus, further investigations are required to clarify the reaction pathway in more detail for the present system.

3.3. Effect of the Substrate Concentration. To examine the influence of the ethanol concentration on the product formation, oxidation experiments with different initial concentrations were performed (Figures 3a and 3b).

Only minor and irregular difference in catalyst performance was observed when the concentration of ethanol was changed gradually from 2.5 to 50 wt % (with constant catalyst to substrate ratio) (Figure 3a). This clearly showed that the concentration affected the yield much less than the oxidant pressure and reaction temperature, indicating that the reaction was not kinetically controlled under the applied reaction conditions. By variation of the catalyst to ethanol ratio (Figure 3b) a tendency of increased conversion and acetic acid yield in the order 2 wt % > 5 wt % > 10 wt % was observed, thus confirming the catalytic nature of the added catalyst. Summarizing the results from Figures 3a and 3b, it is obvious that the catalytic system is applicable for a wide range of alcohol concentrations, thus making it prone to be utilized for various applications, including fermented bioethanol oxidation.

3.4. Reference Experiments with Ru(OH)_x/CeO₂. As cerium oxide-supported ruthenium catalysts exhibited improved activity compared to titania, alumina, and spinel catalysts, additional experiments were conducted to investigate their performance.

The results in Table 4 suggest that the support itself (i.e., pristine CeO₂) had low but not negligible catalytic activity. Hence, the conversion of ethanol after 3 h of reaction time increased from 11%, when no catalyst or support was introduced to the reaction (Table 4, entry 1), to 17% in presence of CeO₂ (entry 2), while the product formation increased accordingly. The catalytic activity of the support is possibly related to the redox

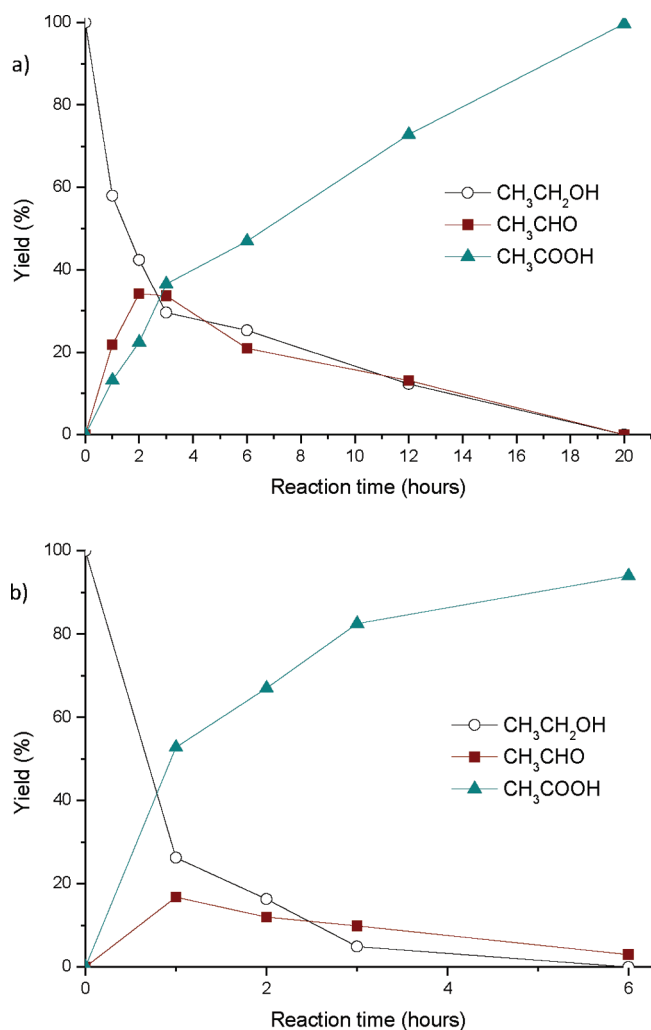


Figure 2. Product yields in the aerobic oxidation of aqueous ethanol with 2.4 wt % Ru(OH)_x/CeO₂ catalyst at (a) 150 °C and (b) 200 °C (10 g of 5 wt % aqueous ethanol, 0.23 mol % Ru, 10 bar O₂).

activity of cerium(IV) oxide usually ascribed to the Ce⁴⁺/Ce³⁺ redox interactions on its surface.^{35–37} The oxidation in inert atmosphere (Table 4, entry 5) appeared to be negligible, as anticipated. The small amount of the formed oxidation product (in addition to the contribution from CeO₂) most likely originated from the remaining oxygen dissolved in the reaction solution because of insufficient removal when saturated with argon prior to the experiment. Good catalytic activity was only observed with the catalyst containing ruthenium (Table 4, entries 3 and 4), thus confirming most of the catalytic activity to originate from the metal inventory.

To obtain information about the product stability, an experiment was also carried out at prolonged reaction time (Table 4, entry 4). After 90 h of continuous reaction, the product (acetic acid) was exclusively formed and remained stable, as indicated by the almost negligible difference (ca. 2%) between conversion and yield.

3.5. Effect of the Ru(OH)_x Loading on Supports. To elucidate the effect of the loading of the catalytic active ruthenium on the surface of cerium oxide, 0.6 wt %, 1.2 wt %, 2.4 wt %, and 4.7 wt % Ru(OH)_x/CeO₂ catalysts were also tested in the aerobic oxidation of ethanol (Figures 4 and 5, Table 5).

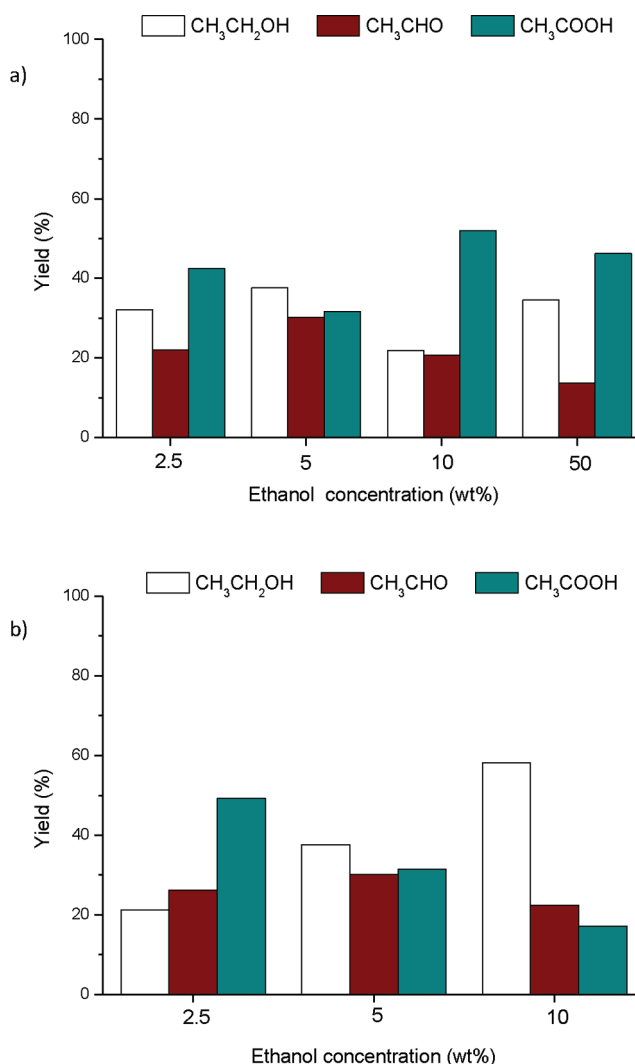


Figure 3. Product distribution in the aerobic oxidation of aqueous ethanol with 2.4 wt % Ru(OH)_x/CeO₂ catalyst at (a) constant catalyst to substrate ratio (0.23 mol %) and (b) constant added amount of catalyst (0.105 g) (10 g of aqueous ethanol solution, 150 °C, 10 bar O₂, 3 h reaction time).

First, performance of the catalysts with different Ru(OH)_x loadings was compared (Figure 4). The mass of the catalyst was altered in the four experiments so the Ru amount (relative to substrate) remained constant at 0.23 mol %.

Change of the ruthenium loading from 0.6 to 4.7 wt % on ceria gradually decreased catalyst activity; the usage of 0.6 wt % catalyst provided full conversion, whereas the conversion with 4.7 wt % Ru(OH)_x/CeO₂ reached only about 50%. This may possibly be explained by the different particle sizes found in the ceria-supported catalysts (see Table 1). Higher ruthenium loading resulted in larger particles, and hence in a decrease of the number of active sites, which in turn decreased the activity of the catalyst.

Also, the extraordinary properties of ceria as surface oxygen capacitor³⁷ and the inherent catalytic activity of CeO₂ in the oxidation (as was shown in Table 4) might facilitate the oxidation as more ceria is introduced in the reaction when the same substrate to catalyst ratio is used (i.e., 0.21 g of 1.2 wt % Ru(OH)_x/CeO₂ corresponded to 0.05 g of 4.7 wt % Ru(OH)_x/CeO₂).

Table 4. Results of the Aerobic Oxidation of Aqueous Ethanol with Supported 2.4 wt % Ru(OH)_x Catalysts^a

entry	catalyst	reaction time (hours)	gas/pressure (bar)	conversion (%)	yield (%)	
					CH ₃ CHO	CH ₃ COOH
1		3	O ₂ /10	11	2	3
2 ^b	CeO ₂	3	O ₂ /10	17	7	9
3	Ru(OH) _x /CeO ₂	3	O ₂ /10	63	30	31
4	Ru(OH) _x /CeO ₂	90	O ₂ /10	>99	0	97
5	Ru(OH) _x /CeO ₂	3	Ar/10	13	4	4

^aReaction conditions: 10 g of 5 wt % aqueous ethanol, 0.23 mol % Ru (entries 3–5), 150 °C. ^bCeO₂ support alone.

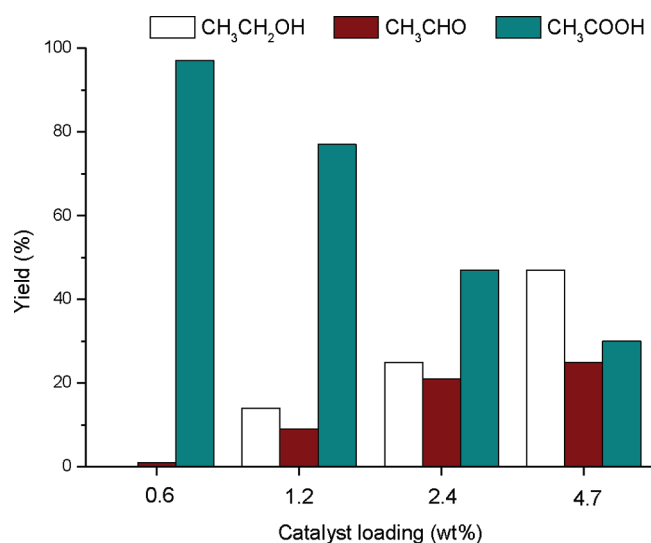


Figure 4. Product distribution in the aerobic oxidation of aqueous ethanol with Ru(OH)_x/CeO₂ catalysts (10 g of 5 wt % aqueous ethanol, 0.23 mol % Ru, 10 bar O₂, 150 °C, 6 h reaction time).

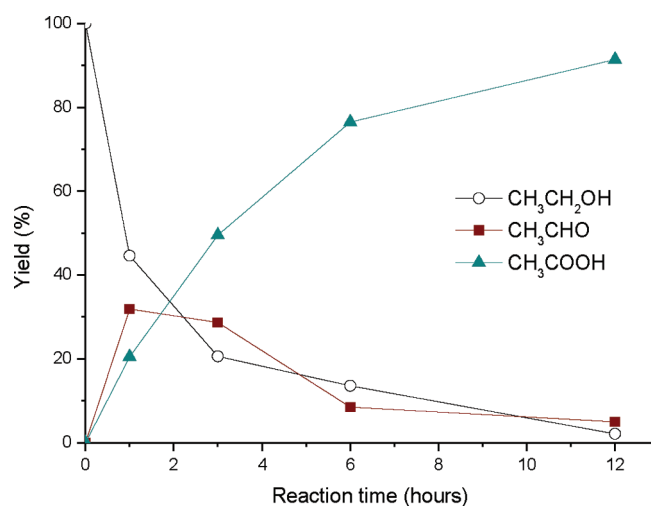


Figure 5. Product yields in the aerobic oxidation of aqueous ethanol with 1.2 wt % Ru(OH)_x/CeO₂ catalyst (10 g of 5 wt % aqueous ethanol, 0.23 mol % Ru, 10 bar O₂, 150 °C).

To further elucidate the loading effect on ceria support, the results obtained with 0.42 g of 0.6 wt % Ru(OH)_x/CeO₂ (entry 1) can be directly compared to the results using 0.21 g of 1.2 wt % Ru(OH)_x/CeO₂ with added 0.21 g of CeO₂ (entry 2), that is, both Ru mol % and support amount remained constant at the two different catalyst loadings. Virtually no difference in the products yields was observed, supporting the hypothesis that both ceria and Ru(OH)_x contributed to the overall catalyst

activity. However, when similar experiments were performed with 2.4 and 4.7 wt % Ru(OH)_x/CeO₂ catalysts (0.23 mol % Ru, overall mass 0.42 g) (Table 5, entries 3 and 4), it was found that both substrate conversion and product yields were significantly lower, even with added CeO₂, and that the catalyst performance was lower than compared to the catalysts with lower loadings. In other words, the rate of the reaction was lower with higher catalyst loading than with lower loading. This result was in accordance with the findings discussed above (see Figure 4). Thus, for the Ru(OH)_x/CeO₂ catalyst, at least some of its improved performance with lower Ru(OH)_x loading originated from the increased support amount. However, after reaching some optimal loading (apparently about 1 wt % Ru(OH)_x) the change in the particle size becomes negligible and less important compared to the contribution in activity obtained from the increased amount of added CeO₂ to the overall performance of the CeO₂-supported catalysts.

Interestingly, the decrease of the ruthenium loading on spinel did not significantly improve the results for the oxidation with spinel-supported Ru(OH)_x catalysts (Table 5, entries 5 and 6). As shown above, MgAl₂O₄, and especially with the deposited ruthenium, has higher surface area than CeO₂ (see Table 1, entries 5–12). Therefore, the obtained results suggest that a small variation in loading of the active species on spinel did not affect the particles size. Comparison of the activity of cerium oxide- and spinel-supported catalysts with 1.2 wt % Ru(OH)_x (entries 5 and 7) exhibiting the same particle size range of ~0.5–2 nm (see Table 1, entries 6 and 10), demonstrated the former to be significantly more active yielding about 50% higher conversion and product yields. This unambiguously confirmed CeO₂ to be the preferred support for the oxidation under the examined reaction conditions.

A catalyst reuse experiment was also conducted with a cerium oxide-supported catalyst. Here the reaction was first performed with 1.2 wt % Ru(OH)_x/CeO₂ catalyst for 3 h, then the catalyst was filtered off, washed with hot water, dried at 140 °C for 2 h, and utilized in another reaction (Table 5, entries 7 and 8). The obtained data confirmed that the catalyst was prone to reuse under the applied reaction conditions. Similar result was also previously found for Ru(OH)_x supported on CeO₂ and MgAl₂O₄ when applied for the catalytic aerobic oxidation of 5-hydroxymethylfurfural in water under elevated pressures and temperatures.^{30,31}

As the preliminary test showed that the 1.2 wt % ceria-supported ruthenium catalyst exhibited superior performance compared to the 2.4 wt % catalyst as well as to the 1.2 and 2.4 wt % spinel-supported catalysts (Table 5), a time study of the reaction with the former catalyst was conducted (Figure 5). This study clearly confirmed that the 1.2 wt % catalyst exhibited higher activity than the 2.4 wt % catalyst under the same reaction conditions (see Figure 2a for comparison), allowing to obtain acetic acid yield above 90% after 12 h of reaction time.

Table 5. Results of the Aerobic Oxidation of Aqueous Ethanol with Supported Ru(OH)_x Catalysts^a

entry	catalyst	reaction time (hours)	conversion (%)	yield (%)	
				CH ₃ CHO	CH ₃ COOH
1 ^b	0.6 wt % Ru(OH) _x /CeO ₂	1	65	33	32
2 ^c	1.2 wt % Ru(OH) _x /CeO ₂ , CeO ₂	1	63	30	31
3 ^d	2.4 wt % Ru(OH) _x /CeO ₂ , CeO ₂	1	54	30	23
4 ^e	4.7 wt % Ru(OH) _x /CeO ₂ , CeO ₂	1	39	18	19
5	1.2 wt % Ru(OH) _x /MgAl ₂ O ₄	3	45	15	27
6	2.4 wt % Ru(OH) _x /MgAl ₂ O ₄	3	41	14	22
7	1.2 wt % Ru(OH) _x /CeO ₂	3	71	27	43
8	1.2 wt % Ru(OH) _x /CeO ₂ (reuse)	3	70	24	42

^aReaction conditions: 10 g of 5 wt % aqueous ethanol, 0.23 mol % Ru, 10 bar O₂, 150 °C. ^b0.42 g of 0.6 wt % Ru(OH)_x/CeO₂. ^c0.21 g of 1.2 wt % Ru(OH)_x/CeO₂ with added 0.21 g of CeO₂. ^d0.11 g of 2.4 wt % Ru(OH)_x/CeO₂ with added 0.31 g of CeO₂. ^e0.05 g of 4.7 wt % Ru(OH)_x/CeO₂ with added 0.37 g of CeO₂.

3.6. Leaching Test. Although the recovered catalyst proved to be reusable under the applied reaction conditions (see Table 5, entry 8), additional experiments were conducted to exclude any homogeneous catalytic contribution or lixiviation of catalytic species in the catalyzed reaction.

First, ICP analysis of the postreaction mixture with 1.2 wt % Ru(OH)_x/CeO₂ (10 bar O₂, 150 °C, 12 h of reaction time; see Figure 5) was conducted. The result revealed a concentration of Ruⁿ⁺ ions after the reaction corresponding to a negligible catalyst leaching (<0.02%).

Second, a reaction was carried out with the catalyst at 150 °C under 10 bar of O₂ for 1 h, where after the catalyst was filtered off and the filtrate poured back into the reactor autoclave. The reactor was then repressurized with 10 bar O₂ and the reaction continued for additional 2 h (Figure 6). No ethanol conversion

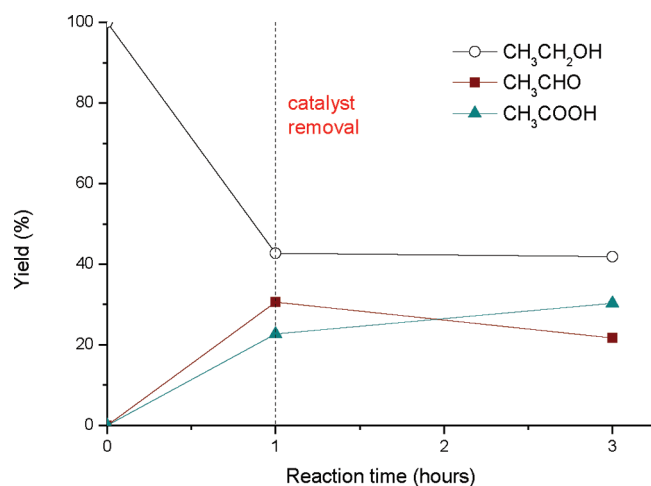


Figure 6. Product yields in the aerobic oxidation of aqueous ethanol with 1.2 wt % Ru(OH)_x/CeO₂ catalyst (10 g of 5 wt % aqueous ethanol, 0.23 mol % Ru, 150 °C, 10 bar O₂).

occurred after the catalyst was removed (i.e., no catalytic species dissolved), while a certain amount of aldehyde was converted into the acid. It is known that aerobic oxidation of aldehydes to carboxylic acids can proceed to some extent even without added catalyst under atmospheric oxygen pressure³⁸ and therefore it can be expected to occur under the reaction conditions here as well.

As an additional experiment, the oxidation reaction was further performed at the same conditions with acetaldehyde as the substrate. The 1.2 wt % Ru(OH)_x/CeO₂ (0.23 mol % Ru) cata-

lyst was here mixed with 10 g of 5 wt % acetaldehyde solution in water at 150 °C and 10 bar of O₂. After a reaction time of 3 h, the yield of acetic acid constituted 86% with 10% of acetaldehyde remaining unconverted. This result, compared with the data from Table 5 and Figures 5 and 6, indicates that the initial oxidation of ethanol to acetaldehyde is the performance determining step in the overall reaction sequence.

3.7. Effect of the Catalyst Calcination Temperature. To examine the effect of the catalyst calcination on catalytic performance, results from the oxidation reaction with a non-treated catalyst were compared to results obtained with the catalysts calcined at two different temperatures (Figure 7).

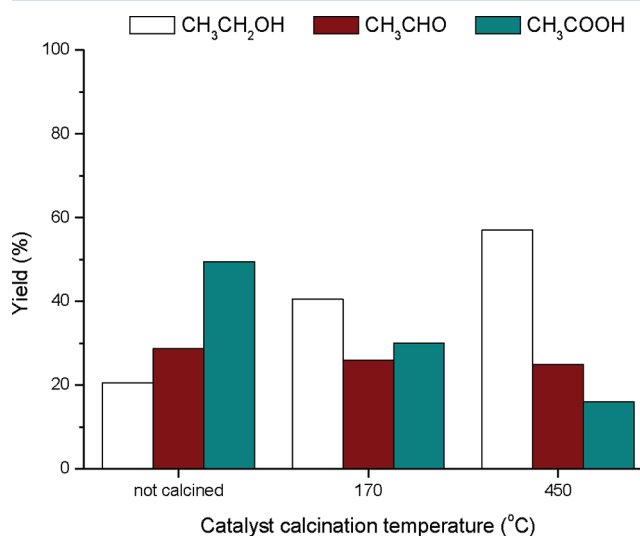


Figure 7. Product yields in the aerobic oxidation of aqueous ethanol with noncalcined (dried at 140 °C) and calcined 1.2 wt % Ru(OH)_x/CeO₂ catalysts (10 g of 5 wt % aqueous ethanol, 0.23 mol % Ru, 150 °C, 10 bar O₂, 3 h reaction time).

As shown in Figure 7, the calcination temperature affected the activity of the catalyst. Hence, within 3 h of reaction the calcined catalysts proved less active than the noncalcined catalyst resulting in decreased ethanol conversion and acetic acid yield, although the yield of acetaldehyde remained virtually the same. Moreover, both substrate conversion and acetic acid yield decreased with increase of the catalyst calcination temperature suggesting possible changes in, for example, oxidation state or crystallinity of Ru-species already with moderate temperature changes.

XRPD and TEM images were recorded of the 1.2 wt % Ru(OH)_x/CeO₂ catalyst after calcination at 450 °C (Supporting Information, Figures S1 and S2) and compared to the non-calcined catalyst to determine differences in the Ru-particles. As anticipated, no formation of crystalline Ru-species could be confirmed by XRD after calcination with this low Ru loading, but TEM established that the initially formed small particles (see Figure 1b) were not present after calcination. This clearly suggested particle sintering to occur upon heating, though larger particles were difficult to differentiate from the support crystallites.

In summary, these observations are in good accordance with the results reported by Yu et al.³⁹ where a decrease in the aerobic catalyst performance was ascribed to dehydration of ruthenium species, when hydrated ruthenium oxide catalytic species were annealed in N₂ at high temperatures. Moreover, heat-induced particle sintering for supported RuO_x catalysts, accompanied by the formation of crystalline RuO₂ from initially amorphous²⁸ ruthenium species, have also recently been reported by Chorkendorff and co-workers.⁴⁰

4. CONCLUSIONS

Highly selective and efficient aerobic oxidation of aqueous ethanol (2.5–50 wt %) to acetic acid with supported ruthenium hydroxide catalysts at elevated temperatures and oxygen pressures was reported. Under the applied reaction conditions a change in ethanol concentration had only minor effect on the yields. However, a temperature of 125 °C or higher was needed to give high yield of acetic acid. At temperatures about 200 °C, over oxidation of the ethanol was observed leading to lower acetic acid selectivity and yields.

The performance of catalysts based on different supports increased in the order Ru(OH)_x/TiO₂ < Ru(OH)_x/Al₂O₃ < Ru(OH)_x/MgAl₂O₄ < Ru(OH)_x/CeO₂ when applying identical reaction conditions. Furthermore, the activity of the CeO₂-supported Ru(OH)_x catalysts was found to be dependent on the ruthenium species loading on the surface of the support. Increases in ruthenium loading gave larger particle sizes, as expected, and thereby lower catalytic activity. The optimal performance was found to occur with approximately 1 wt % Ru(OH)_x loading with a particle size of 0.6–2 nm. Above this loading a decrease of the catalytic activity contributed by ruthenium species was found. Furthermore, calcination of the catalysts gave lower activity which most likely was due to a combination of dehydration and sintering of the small Ru-containing particles.

In conclusion, quantitative yield of acetic acid was obtained with a 1.2 wt % Ru(OH)_x/CeO₂ catalyst at reaction conditions of 150 °C, 10 bar O₂ after 12 h hours of reaction time. Importantly, the oxidation of aqueous ethanol solutions of high concentrations was shown to proceed with similar efficiency using Ru(OH)_x/CeO₂ catalysts, thus providing an opportunity for utilization of the catalyst systems in bioethanol upgrading.

■ ASSOCIATED CONTENT

Supporting Information

X-ray powder diffraction patterns and TEM images of catalysts. This material is available free of charge via the Internet at <http://pubs.acs.org>.

■ AUTHOR INFORMATION

Corresponding Author

*E-mail: ar@kemi.dtu.dk. Phone: +4545252233. Fax: +4545883136.

Notes

The authors declare no competing financial interest.

■ ACKNOWLEDGMENTS

The authors thank Bodil F. Holten, Centre for Catalysis and Sustainable Chemistry, for BET measurements. The A. P. Møller and Chastine Mc-Kinney Møller Foundation is gratefully acknowledged for its contribution towards the establishment of the Center for Electron Nanoscopy at the Technical University of Denmark.

■ REFERENCES

- (1) Weissmehl, K.; Arpe, H.-J. *Industrial Organic Chemistry*, 4th ed.; Wiley-VCH: Weinheim, Germany, 2003; p 171.
- (2) Ebner, H.; Follmann, H.; Sellmer, S. Vinegar. In *Ullmann's Encyclopedia of Industrial Chemistry*, 7th ed.; Wiley-VCH: Weinheim, Germany, 2005.
- (3) Simpson, T. W.; Sharpley, A. N.; Howarth, R. W.; Paerl, H. W.; Mankin, K. R. *J. Environ. Qual.* **2008**, *37*, 318–24.
- (4) Rass-Hansen, J.; Falsig, H.; Jørgensen, B.; Christensen, C. H. *J. Chem. Technol. Biotechnol.* **2007**, *82*, 329–333.
- (5) Hirashima, S.; Itoh, A. *Green Chem.* **2007**, *9*, 318–320.
- (6) Wolfel, R.; Taccardi, N.; Bosmann, A.; Wasserscheid, P. *Green Chem.* **2011**, *13*, 2759–2763.
- (7) Zotova, N.; Hellgardt, K.; Kelsall, G. H.; Jessiman, A. S.; Hü, K. K. *Green Chem.* **2010**, *12*, 2157–2163.
- (8) Cheung, H.; Tanke, R. S.; Torrence, G. P. Acetic acid. In *Ullmann's Encyclopedia of Industrial Chemistry*, 7th ed.; Wiley-VCH: Weinheim, Germany, 2005.
- (9) Thomas, C. *Coord. Chem. Rev.* **2003**, *243*, 125–142.
- (10) Kamble, D. L.; Nandibewoor, S. T. *J. Phys. Org. Chem.* **1998**, *11*, 171–176.
- (11) Nielsen, I. S.; Taarning, E.; Egeblad, K.; Madsen, R.; Christensen, C. H. *Catal. Lett.* **2007**, *116*, 35–40.
- (12) Han, J.; Liu, Y.; Guo, R. *Adv. Funct. Mater.* **2009**, *19*, 1112–1117.
- (13) Rajesh, H.; Ozkan, U. S. *Ind. Eng. Chem. Res.* **1993**, *32*, 1622–1630.
- (14) Li, X.; Iglesia, E. *Chem.—Eur. J.* **2007**, *13*, 9324–9330.
- (15) ten Brink, G.-J.; Arends, I. W. C. E.; Sheldon, R. A. *Science* **2000**, *287*, 1636–1639.
- (16) Nishimura, T.; Kakiuchi, N.; Inoue, M.; Uemura, S. *Chem. Commun.* **2000**, 1245–1246.
- (17) Mori, K.; Hara, T.; Mizugaki, T.; Ebitani, K.; Kaneda, K. *J. Am. Chem. Soc.* **2004**, *126*, 10657–10666.
- (18) Nagai, M.; Gonzalez, R. D. *Ind. Eng. Chem. Prod. Res. Dev.* **1985**, *24*, 525–531.
- (19) Takei, T.; Iguchi, N.; Haruta, M. *Catal. Surv. Asia* **2011**, *15*, 80–88.
- (20) Christensen, C. H.; Jørgensen, B.; Rass-Hansen, J.; Egeblad, K.; Madsen, R.; Klitgaard, S. K.; Hansen, S. M.; Hansen, M. R.; Andersen, H. C.; Riisager, A. *Angew. Chem., Int. Ed.* **2006**, *45*, 4648–4651.
- (21) Jørgensen, B.; Christiansen, S. E.; Thomsen, M. L. D.; Christensen, C. H. *J. Catal.* **2007**, *251*, 332–337.
- (22) Yamaguchi, K.; Mizuno, N. *Angew. Chem., Int. Ed.* **2002**, *41*, 4538–4542.
- (23) Kotani, M.; Koike, T.; Yamaguchi, K.; Mizuno, N. *Green Chem.* **2006**, *8*, 735–741.
- (24) Kim, J. W.; Yamaguchi, K.; Mizuno, N. *Angew. Chem., Int. Ed.* **2008**, *47*, 9249–9251.
- (25) Mizuno, N.; Yamaguchi, K. *Catal. Today* **2008**, *132*, 18–26.
- (26) Yamaguchi, K.; Mizuno, N. *Synlett* **2010**, *16*, 2365–2382.
- (27) Zhang, Y.; Xu, K.; Chen, X.; Hu, T.; Yu, Y.; Zhang, J.; Huang, J. *Catal. Commun.* **2010**, *11*, 951–954.

- (28) Taarning, E.; Nielsen, I. S.; Egeblad, K.; Madsen, R.; Christensen, C. H. *ChemSusChem* **2008**, *1*, 75–78.
- (29) Gorbanev, Y. Y.; Klitgaard, S. K.; Woodley, J. M.; Christensen, C. H.; Riisager, A. *ChemSusChem* **2009**, *2*, 672–675.
- (30) Gorbanev, Y. Y.; Kegnæs, S.; Riisager, A. *Top. Catal.* **2011**, *54*, 1318–1324.
- (31) Gorbanev, Y. Y.; Kegnæs, S.; Riisager, A. *Catal. Lett.* **2011**, *141*, 1752–1760.
- (32) Imamura, S.; Fukuda, I.; Ishida, S. *Ind. Eng. Chem. Res.* **1988**, *27*, 718–721.
- (33) Liu, H.; Iglesia, E. *J. Phys. Chem. B* **2005**, *109*, 2155–2163.
- (34) Nikaidou, F.; Ushiyama, H.; Yamaguchi, K.; Yamashita, K.; Mizuno, N. *J. Phys. Chem. C* **2010**, *114*, 10873–10880.
- (35) Pavasupree, S.; Suzuki, Y.; Pivsa-Art, S.; Yoshikawa, S. *J. Solid State Chem.* **2005**, *178*, 128–134.
- (36) Magesh, G.; Viswanathan, B.; Viswanath, R. P.; Varadarajan, T. K. *Indian J. Chem., Sect. A* **2009**, *48A*, 480–488.
- (37) Vayssilov, G. N.; Lykhach, Y.; Migani, A.; Staudt, T.; Petrova, G. P.; Tsud, N.; Skála, T.; Bruix, A.; Illas, F.; Prince, K. C.; Matolin, V.; Neyman, K. M.; Libuda, J. *Nat. Mater.* **2011**, *10*, 310–315.
- (38) Larkin, D. R. *J. Org. Chem.* **1990**, *55*, 1563–1568.
- (39) Yu, H.; Zeng, K.; Zhang, Y.; Peng, F.; Wang, H.; Yang, J. *J. Phys. Chem. C* **2008**, *112*, 11875–11880.
- (40) Kleiman-Shwarsstein, A.; Laursen, A.; Cavalca, F.; Tang, W.; Dahl, S.; Chorkendorff, I. *Chem. Commun.* **2012**, *48*, 967–969.